Abstract: Arsenic trioxide (ATO, As_2O_3) is currently used to treat acute promyelocytic leukemia. However, expanding its use to include high-dose treatment of other cancers is severely hampered by serious side effects on healthy organs. To address these limitations, we loaded ATO onto folate (FA)-labeled human serum albumin (HSA) pretreated with glutathione (GSH) based on the low pH- and GSH-sensitive arsenic-sulfur bond, and we termed the resulting smart nanodrug as FA-HSA-ATO. FA-HSA-ATO could specifically recognize folate receptor-β-positive chronic myeloid leukemia (CML) cells, resulting in more intracellular accumulation of ATO. Furthermore, the nanodrug could upregulate FRβ expression in CML cancer cells and xenograft tumor model, facilitating even more recruitment and uptake of FRβ-targeting drugs. *In vitro* and *in vivo* experiments indicate that the nanodrug significantly alleviates side effects and improves therapeutic efficacy of ATO on CML and xenograft tumor model.

DOI: 10.1002/anie.2016XXXXX

Table of Contents

Materials and methods

Reagents. Human serum albumin (HSA), As_2O_3 (Arsenic trioxide, ATO), phosphotungstic acid, glutathione (GSH), 3-(4,5-dimethylthiazol-2-yl)-2,5-diphenyltetrazolium bromide (MTT), and N-hydroxysuccinimide ester of fluorescein isothiocyanate were obtained from Sigma-Aldrich (St. Louis, MO). Anti-FR-β (F0LR2) and Ki67 antibody were purchased from Abcam (Cambridge, United Kingdom). Annexin V-FITC/Propidium Iodide (PI) Cell Apoptosis Kit was obtained from Beyotime (Nantong, China). Dulbecco's phosphate-buffered saline (D-PBS, pH 7.4), fetal bovine serum (FBS), folate-free RMPI 1640, folate-free DMEM, trypsin-EDTA and penicillin-streptomycin were purchased from Gibco Life Technologies (AG, Switzerland). Folic acid (folate, FA) and paclitaxel (PTX) were purchased from Huateng Pharma Co., Ltd. (Changsha, China). DPPC, Chol, DPPE-PEG_{2000}, DSPE-PEG_{3350}-Folate and FITC-PEG-FA (FITC-PEG_{2000}-FA, MW: 2000) were purchased from Ponsure Biotechnology (Shanghai, China). Dialysis bag with a molecular weight cutoff of 8-14 kDa was bought from Millipore (USA). All solutions were prepared using ultrapure water, which was prepared through a Millipore Milli-Q water purification system (Billerica, MA, USA) with an electrical resistance >18.3 MΩ. All other chemicals used in this study were of analytical reagent grade and used without further purification. BALB/c athymic nude mice and BALB/c mice were maintained under aseptic conditions in a small animal isolator. All food, water, bedding and cages were autoclaved before use.

Cell culture and buffer. K562, K562/ADR, HL-60, U937, CCRF-CEM, Ramos, HeLa, A549 and H1299 cells were purchased from ATCC (Bethesda, MD, USA) and were cultured in DMEM or RPMI 1640 media (Gibco) supplemented with 10% (v/v) fetal bovine serum (FBS, Gibco) and 1 x antibiotics (Gibco) at 37 ℃ in 5% CO_2 atmosphere. Fresh leukemia mononuclear cells from peripheral blood of 15 AML (acute myelogenous leukemia), 8 ALL (acute lymphoblastic leukemia) and 16 CML (chronic myeloid leukemia) leukemia patients, who were classified according to the French–American–British (FAB) classification system, as well as 9 healthy donors, were enriched by Ficoll separation. Informed consent was obtained according to institutional guidelines. Mononuclear cells were suspended in RPMI 1640 medium containing 10% FBS at a density of approximately 5-10 × 10^5/mL for treatment. Dulbecco's phosphate buffered saline without Ca^{2+} and Mg^{2+} (D-PBS, Invitrogen) was used to wash cells.

Apparatus. Dynamic light scattering was measured on a Malvern Zetasizer Nano ZS90 (Malvern Instruments, Ltd., Worcestershire, UK). Transmission electron microscopy (TEM) images were obtained on a H-7000 NAR transmission electron microscope (Hitachi) with a working voltage of 100 kV. UV-Vis spectral analysis was carried out on a UV-2450 UV-vis spectrophotometer (Shimadzu). Circular dichroism (CD) spectra were recorded on a Bio-Logic MOS-500 instrument at 25 ℃. The concentration of arsenic was quantified through inductively coupled plasma optical emission spectrometry (Optima 8000 ICP-OES spectrometer, Perkin-Elmer). Flow cytometry analysis of cells was performed on a BD FACSVerse™ flow cytometer (BD Biosciences, Ann Arbor, MI). Fluorescence images of cells were collected on a FV1000-X81 confocal microscope (Olympus, Japan) and analyzed by FV10-ASW, version 3.1. Fluorescence images of live mice were collected by an IVIS Lumina II *in vivo* imaging system (Caliper Life Science, USA). The fluorescence images of tumor sections were collected on a Pannoramic 250 Flash II (3DHISTECH, Hungary).

Preparation of folate-labeled HSA, FITC-labeled HSA and folate/FITC-labeled HSA. N-hydroxysuccinimide ester of folate (folate-NHS) was prepared according to a procedure reported previously[1]. To prepare FA-HSA and FITC-HSA, either folate-NHS (approximately 10 mg) or fluorescein isothiocyanate (Sigma, 2.5 mg) was dissolved in 1 mL carbonate/bicarbonate buffer (0.1 M, pH = 9) and then added with stirring to 4 mL of 25 mg/mL HSA solution. The reaction was maintained for 180 minutes at ambient temperature in the dark. At a predetermined time, the pH of the reacted solution was adjusted 7 ~ 8 using 0.1 M HCl. Excess reactants and byproducts were removed using Sephadex G-50. The elution supernatant, FA-HSA or FITC-HSA, was lyophilized and saved for use. FA/FITC-HSA was prepared by conjugating FA-HSA (120 mg) with fluorescein isothiocyanate (2.5 mg), followed by dialysis (MWCO 8-14 KD) against 10 mM PBS at 4 ℃ for 24 h.

Determination of coupling ratio. Since spectra of HSA, FA, and FITC had UV-vis absorption peaks at 280 nm, 363 nm and 495 nm, respectively, a UV-vis spectrophotometer was used to determine the content of HSA, FA, and FITC in the FA-HSA and FA/FITC-HSA conjugates. HSA concentration was calculated as Y = 0.418X + 0.120, R^2 = 0.9998 (Y, HSA concentration in mg/mL; X, absorbance). The concentration of folate conjugated with HSA was calculated according to standard curve (Y = 0.014X + 0.176, R^2 = 0.9999, Y,

folate concentration in μg/mL; X, absorbance) generated by serial concentrations of folate. The ratio of FITC to HSA was calculated as FITC/HSA= $3.1\times A_{495}/[A_{280}-0.31\times A_{495}]$.

Preparation of various HSA-ATO nanodrugs. HSA, equivalent to FA-HSA or FA/FITC-HSA, was dissolved in 1 mL of D-PBS at the concentration of 50 mg/mL and then treated with 60 mM GSH at 37 ℃ to break up the intramolecular disulfide bonds and expose free sulfhydryl groups. After 60 min, 1 mL of As_2O_3 (5 mg/mL, pH 5-6) was added to the GSH-treated HSA solution. The mixture of ATO and HSA was stirred at room temperature for 120 min. The resulting HSA-ATO nanodrug was dialyzed (MWCO 8-14 KD) in D-PBS at 4 ℃ for 24 h to remove excess ATO, GSH and byproduct GSSG and then kept at 4 ℃ for use. Ellman's method was used to monitor the ratio of free sulfhydryl groups in HSA, reduced FA-HSA and FA-HSA-ATO[2]. FA-HSA-ATO was prepared by conjugating ATO with FA-HSA (FA:HSA ≈ 7:1, Table S1), while HSA-ATO nanodrug (hereinafter 'HSA-ATO') was prepared by conjugating ATO with HSA. Conjugation was achieved through the formation of an As^{III}-S bond between arsenic and a free sulfhydryl group in these two HSA formulations pretreated with glutathione (GSH).

Preparation of folate-targeted liposome encapsulating arsenic (f-Lip(Ni, As)). Folate-targeted liposomes encapsulating arsenic was prepared according to a previous method[3]. Briefly, the mixture of DPPC/Chol/DPPE-PEG_{2000}/DSPE-PEG_{3350}-Folate (53/45/1.7/0.3 mol%) in chloroform were evaporated using a rotary evaporator. After completely removing any residual solvent, the resulting dried lipid films were hydrated in 300 mmol/L nickel acetate [$Ni(OAc)_2$] aqueous solutions, followed by 10 freeze-and-thaw cycles (freezing in ethanol/dry ice bath and thawing in 50°C water bath). The hydrated liposomes were then sequentially extruded with a manual mini-extruder (Avanti Lipids) equiped with a series of polycarbonate filters of pore size ranging from 0.4 to 0.1 μm. Extruded $Ni(OAc)_2$ encapsulated liposomes (f-Lip(Ni)) were fractionated on Sephadex G-50 columns equilibrated with a 20 mM HEPES buffer (pH 6.8) containing 150 mM NaCl. f-Lip(Ni) was then incubated with a As_2O_3 solution at 50°C for 2.5 h to prepare folate-targeted liposome encapsulating arsenic (f-Lip(Ni, As)). After cooling to room temperature and removal of extraliposomal As_2O_3 with Sephadex G-50 columns, f-Lip(Ni, As) were characterized with ICP-OES.

Determination of arsenic in FA-HSA-ATO. To determine arsenic loading in FA-HSA-ATO, one milligram of FA-HSA-ATO solution was digested with 1 mL 10% nitric acid in a 50 ℃ water bath overnight. The digested protein solution was then diluted with 19 mL of water and filtered with a 0.45 μm polyvinylidene difluoride (PVDF) filter (Millipore, USA) before ICP-OES analysis. The quantification of arsenic in digested samples was based on arsenic external standard calibration prepared from arsenic containing multi-element ICP-OES calibration standard solutions. The method was evaluated with diluted standard, a certified reference for trace element determination in fresh water. Triplicate independent analyses were performed on all standard solutions and samples.

Characterization of HSA-ATO and FA-HSA-ATO. Freshly prepared HSA, HSA-ATO or FA-HSA-ATO were transferred onto a 200 mesh copper grid coated with carbon, stained with 2% (w/v) phosphotungstic acid, dried at room temperature, and then analyzed by TEM. The size of the freshly prepared sample (1 mg/mL) was also measured by dynamic light scattering (DLS), using a Malvern Zetasizer Nano ZS. Given the sensitivity of the instrument, multiple runs (>3) were performed to avoid erroneous results.

***In vitro* arsenic release and stability studies.** To analyze stability and arsenic release, FA-HSA-ATO samples (750 μM arsenic equivalents) were added to 1 mL of RPMI 1640 cell medium, human serum, and D-PBS buffer with different GSH concentrations (0, 0.01, 1, 5, 10 mM GSH), or acetate buffer (pH 5.5, 6.0, 6.5), and the resulting mixtures were placed in a D-Tube Dialyzer Maxi (MWCO 3.5 kDa, Merck Millipore) for dialysis in a 37 ℃ water bath[4]. At predetermined times, 200 μL of sample were removed from the T-tube for arsenic analysis with ICP-OES (Optima 8000 ICP-OES spectrometer, Perkin-Elmer), and aliquots of buffer were supplemented.

Flow cytometric analysis and confocal microscopy imaging. To analyze the binding of FITC-PEG-FA to cells pretreated with or without ATO or FA-HSA-ATO, the cells were processed according to the following procedure. First, the cells (5×10^6) were washed with 500 μL of acetate buffer (10 mM sodium acetate, pH 4, 150 mM NaCl, 7 mM glucose) at 4 ℃ for 2 minutes to remove endogenously bound folate after pretreatment with ATO or FA-HSA-ATO, followed by 2 washes with 500 μL of D-PBS and incubation

with 10 nM FITC-PEG-FA at 4 ℃ for 30 minutes. Then, the samples were centrifuged, washed twice with 500 μL of D-PBS, and finally resuspended in 500 μL of D-PBS for flow cytometric analysis on the BD FACSVerse™ flow cytometer. To investigate the effect of free folate on the binding of FITC-PEG-FA, all experimental steps were the same as those for flow analysis mentioned above, except that cells were preincubated with 1 μM folate for 10 minutes before the addition of FITC-PEG-FA.

To analyze the *in vitro* FRβ-targeting ability of FA/FITC-HSA-ATO, 5×10^6 K562 cells were incubated with 2 μM FA/FITC-HSA-ATO, 2 μM FITC-HSA-ATO, or 2 μM FA/FITC-HSA-ATO and 2 mM free folate for 4 h at 37 ℃, respectively. The cells were washed three times with 500 μL of D-PBS to remove the unbound nanodrugs and finally resuspended in 500 μL of D-PBS for flow cytometric analysis and imaging with a FV1000-X81 microscope system (Olympus, Japan).

Quantitative analysis of arsenic in cells, cell medium and extracellular nanodrugs. Either 10^7 suspension cells or 5×10^6 adherent cells were exposed to 1 μM ATO, HSA-ATO (equivalent to 1 μM ATO) or FA-HSA-ATO (equivalent to 1 μM ATO) for 6 hours or 24 hours at 37 ℃. For suspension cells, cells and cell media were separated by centrifugation at 800 rpm for 5 min at predetermined time and collected. The collected cell media were treated with 2- to 5-fold volume of ethanol for 10 min to precipitate proteins. After centrifugation (15,000 × g, 20 min), protein pellets were collected for analysis, and the supernatant was collected and vacuum-dried for analysis. For adherent cells, cell media were collected at predetermined time, followed by the protocol described above. The adherent cells were detached with 0.25% trypsin (Gibco) after washing with D-PBS and collected after centrifugation (800 rpm, 5 min). The collected samples (cell pellets, protein pellets and dried cell media) were digested with 1 mL of nitric acid (10%) for measurement of arsenic amounts through ICP-OES (Optima 8000 ICP-OES spectrometer, Perkin-Elmer). All analyses were independently performed in triplicate.

***In vitro* cytotoxicity assay.** The cytotoxicity of ATO, ATO nanodrug and f-Lip(Ni, As) on cancer cells was determined by 3-(4,5-dimethylthiazol-2-yl)-2,5-diphenyltetrazolium bromide (MTT) assay[5]. Briefly, cells ($5\text{-}10 \times 10^3$ per well) were seeded in 96-well plates. After 24-h incubation, the cells were treated with ATO, HSA-ATO or FA-HSA-ATO at different concentrations for 72 h (triplicate wells for each concentration). Then twenty microliters of MTT solution (5 mg/mL in PBS) were added to each well, and the cells were further incubated for 4 h. After centrifugation at 1000 g for 5 minutes, the media were carefully removed. The remaining purple formazan crystals were dissolved with 200 μL of isopropanol containing 0.1 M HCl. After shaking gently, absorbance at 570 nm was measured with a Synergy 2 Multi-Mode Microplate Reader (Bio-Tek, Winooski, VT). All analyses were independently performed in triplicate, and the error bars represent the standard derivations. The IC_{50} was calculated by fitting the data with nonlinear regression analysis using GraphPad Prism 5.01 (GraphPad Software, San Diego, CA).

Apoptosis analysis. Apoptosis in cells was measured after treatment without or with free ATO, FA-HSA-ATO, and FA-HSA-PTX for various concentrations or time intervals, as indicated. HSA-PTX preparation followed the previously reported protocol[6]. The cells were harvested, washed twice with ice-cold D-PBS and then determined with Annexin V-FITC Apoptosis Detection Kit (Beyotime, China) according to the manufacturer's protocol. Analyses were applied on a BD FACSVerse™ flow cytometer (BD Biosciences, CA). Both early apoptotic and late apoptotic cells were calculated in cell death determinations. Each experiment was performed in triplicate.

Western blot. Cells were lysed in 200 μL of WB&IP lysis buffer (1% Triton X-100), including 1 mM PMSF (Beyotime, China). Protein extracts (50 μg) were loaded onto an 8-15% polyacrylamide gel containing SDS, electrophoresed and transferred to a 0.22 μm nitrocellulose membrane (PALL, USA). The membranes were blocked with 5% non-fat dried milk in Tris-buffered saline containing 0.1% Tween 20 (TBST) and incubated overnight at 4 ℃ with the primary antibody. The blots were washed with TBST three times and then probed with HRP-conjugated secondary antibodies for 2 h at room temperature. The immune complexes were visualized using the Phototope-HRP Western Blot Detection System (Pierce, USA) as previously reported[7]. GAPDH was used to ensure equivalent loading of whole cell protein. All data were confirmed by three individual experiments.

Pharmacokinetics study. ATO, HSA-ATO and FA-HSA-ATO (5 mg/kg body weight, ATO equivalents) were i.v. injected into BALB/c healthy mice (n = 4 for each group). At various times after i.v. injection, blood was collected from the tail vein. After centrifugation, the plasma was separated and collected. Then the concentration of arsenic in the plasma samples was measured by ICP-OES according

to a procedure reported previously. Briefly, the collected plasma samples (200 μL) were incubated with 10% nitric acid overnight in a 50 ℃ water bath in the dark to extract arsenic. The mixture was then centrifuged at 15,000 × g for 20 min, and the supernatant was analyzed by ICP-OES.

***In vivo* studies with murine model.** Athymic nude mice (BALB/c, 4 to 5 weeks old) were obtained from the Shanghai Laboratory Animal Center (Shanghai, China). All animal studies were performed according to protocols approved by the Institutional Animal Care and Use Committee (IACUC) of Hunan University. Mice were s.c. implanted with 8-10 × 10^6 K562 cells in the right or left upper flank (day 0). The cells were tested for mycoplasma contamination before implantation. After ~6 days, when the tumor sizes reached about 0.8 cm in diameter, mice were injected i.v. with 200 μL of FITC-HSA-ATO or FA/FITC-HSA-ATO in 100 μL saline, and in vivo fluorescence imaging was conducted at the indicated time points using an IVIS Lumina II in vivo imaging system (Caliper LifeSicence, USA).

To study biodistribution, female BALB/c mice bearing K562 tumors were injected with ATO, HSA-ATO or FA-HSA-ATO (5 mg/kg BW, ATO equivalents) via tail vein. At 12 h post-injection, mice were sacrificed. Tumors and major tissues were collected, weighed, and homogenized with addition of 1:4 (wt/vol) 10% nitric acid in a tissue homogenizer, treated by ultrasonic waves for 2 hours and then placed in a 50 ℃ water bath in the dark. The extracted arsenic from tumor and main organs was quantified with ICP-OES. The results were presented as percentage of injected dose (%ID) per gram of tissue. Values are expressed as means ± SD (n = 3).

For therapeutic assessment, when the size of tumors reached about 0.5-0.6 cm in diameter, BALB/c nude mice were randomized into four groups (n=5 mice/group) and i.p. administered with ATO (5 mg/kg/day), HSA-ATO (equivalent to ATO 5 mg/kg/day), FA-HSA-ATO (equivalent to ATO 5mg/kg/day) or HSA (Control). All injected reagents were dissolved in D-PBS. Tumor volume (V) was calculated using the formula $V = 0.5 \times a \times b^2$, where 'a' and 'b' are the length and width of the tumor, respectively. In each tumor model, the mice were monitored for up to 51 d after implantation until the condition for euthanasia was met, i.e., tumor greater than 1,000 mm^3. On day 51, all surviving mice were sacrificed.

To compare the expression of folate receptor β in K562 tumors, mice treated with nanodrugs or HSA were sacrificed at 10 days after the last administration of various drug formulations according to the above method. The tumors were excised, fixed in formaldehyde and further processed for frozen embedding. For immunostaining, the frozen tumor sections were washed with 500 μL of acetate buffer (10 mM sodium acetate, pH 4, 150 mM NaCl, 7 mM glucose) at 4 ℃ for 2 minutes to remove endogenously bound folate, followed by 2 washes with D-PBS and incubation with 10 nM FITC-PEG-FA at 4 ℃ for 30 minutes. After two washes with D-PBS, the nuclei were stained with DAPI. Then the sections were imaged with a Pannoramic 250 Flash II (3DHISTECH, Hungary).

Results and Discussion

The clinical applications of some antineoplastic agents in cancers have been hampered by their indiscriminate distribution in the body. Nanocarrier-based drug delivery systems can alleviate the problem to some extent by improving preferential accumulation within the tumor via the EPR effect[8]. However, simple accumulation of nanocarrier at the tumor site does not necessarily ensure increased therapeutic efficacy. To do this, nanocarriers must be distributed throughout the tumor and efficiently taken up by cancer cells[9]. In addition, nanocarriers should be stable in circulation, releasing their payload after cellular uptake. Finally, the components of nanocarriers must be safe and biocompatible. In the present study, our nanodrug meets all these criteria for specific ATO delivery. Compared to other strategies for ATO delivery, our nanodrug has several advantages, as discussed below.

Tumor targeting ability. FA-HSA-ATO was developed by loading ATO on an HSA carrier modified with folate through arsenic-sulfur bond. It has been reported that HSA has a long plasma half-life of 19 days and can be preferentially accumulated in tumor. The modification of HSA with folate endows our nanodrug with active FR-β-targeting ability, affording the nanodrug with the ability to distinguish patient-derived CML cancer cells from ALL cancer cells. FR-β-targeting ability could significantly improve the accumulation of intracellular arsenic in FR-β+ cancer cells. More importantly, FA-HSA-ATO could upregulate FR expression in CML cancer cell lines (K562), and even K562 xenograft tumor, allowing these cells to recruit and take up more FR-β-targeting drugs.

Therefore, the FR-β-targeting ability of FA-HSA-ATO significantly increased cytotoxicity of ATO in CML cancer cells and increased the therapeutic index in patient-derived leukemia cancer cells and K562 tumor.

Favorable safety, stability and tumor microenvironment-sensitive profiles. The *in vivo* characteristics of carriers are largely determined by their surface physicochemical properties. Our carrier consists of FA and HSA, which exist naturally in the human body. Thus, the carrier does not contain any potentially toxic elements that would activate inflammatory or immunological responses; therefore, it is biocompatible and safe when used *in vivo*. FA-HSA-ATO has good serum stability (< 15 % release of ATO within 24 hours at 37 °C) and attenuates the toxicity relative to free ATO. FA-HSA-ATO has a significantly prolonged circulation compared to free ATO (such as $t_{1/2\beta}$ = 9.71 h *vs*. $t_{1/2\beta}$ = 4.27 h for free ATO), high drug accumulation in tumors (6-fold higher than that in free ATO-treated mice and 1.5-fold higher than that in mice treated with HSA-ATO), and less exposure of normal organs to the drug. After extravasation, the size decrease of FA-HSA-ATO responsive to the change of pH from 7.4 to 6.5 (Figure. S5), and the size of FA-HSA-ATO is less than 20 nm (Figure S4), which is ideal for an anticancer nanomedicine because it can fully overcome the physiological barriers imposed by tumor interstitial fluid pressure and actively make its way deep into the tumor tissues[9a]. These properties of FA-HSA-ATO largely improve the therapeutic efficiency of ATO, while reducing its toxic side effects.

In summary, we have shown a smart FA-HSA-ATO nanodrug that expands the use of ATO from APL treatment to CML treatment. The nanodrug was simply prepared by loading ATO on folate-modified HSA through low pH- and GSH-sensitive As^{III}-S bonds. *In vitro* and *in vivo* experiments proved that FA-HSA-ATO with self-amplified FR-β-targeting ability could significantly enhance intracellular arsenic accumulation and prolong the circulation time of ATO, resulting in improved therapeutic index and alleviation of side effects in the treatment of CML K562 tumor. Based on the appealing performance demonstrated in the present study, the overexpression of FR-β in many cancers and their metastatic stroma (e.g., ovarian cancer, liver cancer and lung cancer)[10], as well as the nature of carrier moiety and target moiety, FA-HSA-ATO is expected to be a promising candidate to push the application of ATO from APL to CML, as well as other cancers.

References

[1] C.P. Leamon, P.S. Low, *Proc. Natl. Acad. Sci. USA* **1991**, 88, 5572-5576.

[2] C.K. Riener, G. Kada, H.J. Gruber, *Anal. Bioanal. Chem.* **2002**, 373, 266-276.

[3] H. Chen, R. Ahn, J. Van den Bossche, D. H. Thompson, T. V. O'Halloran, *Mol. Cancer Ther.* **2009**, 8, 1955-1963.

[4] Q. Zhang, M.R. Vakili, X.F. Li, A. Lavasanifar, X.C. Le, *Biomaterials* **2014**, 35, 7088-7100.

[5] X.Q. Pan, X. Zheng, G. Shi, H. Wang, M. Ratnam, R.J. Lee, *Blood* **2002**, 100, 594-602.

[6] Q. Chen, C. Liang, C. Wang, Z. Liu, *Adv. Mater.* **2015**, 27, 903-910.

[7] Q. Liu, Y.B. Peng, P. Zhou, L.W. Qi, M. Zhang, N. Gao, E.H. Liu, P. Li, *Mol. Cancer* **2013**, 12, 135.

[8] a) R. Namgung, Y. Mi Lee, J. Kim, Y. Jang, B.H. Lee, I.S. Kim, P. Sokkar, Y.M. Rhee, A.S. Hoff-man, W.J. Kim, *Nat. Commun.* **2014**, 5, 3702. b) Y. Li, T.Y. Lin, Y. Luo, Q. Liu, W. Xiao, W. Guo, D. Lac, H. Zhang, C. Feng, S. Wachsmann-Hogiu, J.H. Walton, S.R. Cherry, D.J. Rowland, D. Kukis, C. Pan, K.S. Lam, *Nat. Commun.* **2014**, 5, 4712. c) J. Bhattacharyya, J.J. Bellucci, I. Weitzhandler, J.R. McDaniel, I. Spasojevic, X. Li, C.C. Lin, J.T. Chi, A. Chilkoti, *Nat. Commun.* **2015**, 6, 7939. d) G. Zhu, J. Zheng, E. Song, M. Donovan, K. Zhang, C. Liu, W. Tan, Proc. *Natl. Acad. Sci. USA* **2013**, 110, 7998-8003.

[9] a) V.P. Chauhan, R.K. Jain, *Nat. Mater.* **2013**, 12, 958-962. b) E. Blanco, H. Shen, M. Ferrari, *Nat. Biotechnol.* **2015**, 33, 941-951. c) Z. Xiao, D. Shangguan, Z. Cao, X. Fang, W. Tan, *Chemistry* **2008**, 14, 1769-1775.

[10] J. Shen, K.S. Putt, D.W. Visscher, L. Murphy, C. Cohen, S. Singhal, G. Sandusky, Y. Feng, D.S. Dimitrov, P.S. Low, *Oncotarget* **2015**, 6, 14700-14709.

Table S1. Conjugation ratio of HSA modification with FA and FITC.

Molar ratio	FA/HSA	FITC/HSA
FA-HSA	7.50 ± 0.57	
FITC-HSA		3.67 ± 0.61
FA/FITC-HSA	7.38 ± 0.48	3.52 ± 0.39

Table S2. The release of arsenic was accompanied by a size decrease of FA-HSA-ATO.

	pH	GSH (mM)	Hydrodynamic diameter size (nm)
FA-HSA-ATO	7.4		43 ± 5.1
	7.4	0.01	42 ± 6.2
	7.4	1.0	28.1 ± 3.2
	7.4	5.0	13.6 ± 2.7
	7.4	10.0	12.8 ± 1.5
	6.5		25.3 ± 3.9
	6.0		15.7 ± 2.3
	5.5		14.8 ± 2.5

Table S3. Analysis of % of arsenic content in cells, cell medium and ethanol-precipitated protein after cells were treated with ATO, HSA-ATO and FA-HSA-ATO for 6 h or 24 h, respectively.

Cell	Time (h)	Drug	Intracellular (%)	Extracellular (%)	Precipitation (%)
K562	6	ATO	2.52 ± 0.58	94.53 ± 0.81	2.95 ± 0.48
		HSA-ATO	4.83 ± 0.26	7.59 ± 0.86	87.58 ± 0.95
		FA-HSA-ATO	12.24 ± 1.52	7.67 ± 1.54	80.09 ± 3.04
	24	ATO	5.13 ± 0.33	91.80 ± 0.55	3.07 ± 0.82
		HSA-ATO	10.49 ± 0.87	10.39 ± 0.84	79.12 ± 0.44
		FA-HSA-ATO	31.04 ± 1.25	10.88 ± 1.28	58.08 ± 2.46
K562/ADR*	6	ATO	1.95 ± 0.19	94.43 ± 0.88	3.61 ± 0.99
		HSA-ATO	4.67 ± 0.40	9.83 ± 0.91	85.50 ± 0.58
		FA-HSA-ATO	11.93 ± 0.28	10.47 ± 0.55	77.60 ± 0.74
	24	ATO	4.14 ± 0.31	92.83 ± 0.89	3.02 ± 0.60
		HSA-ATO	10.05 ± 0.99	12.61 ± 1.33	77.33 ± 0.54
		FA-HSA-ATO	28.71 ± 0.59	10.96 ± 1.34	60.33 ± 0.77
HL-60	6	ATO	1.67 ± 0.49	94.93 ± 0.78	3.40 ± 0.79
		HSA-ATO	3.06 ± 0.66	10.54 ± 0.84	86.39 ± 1.01
		FA-HSA-ATO	6.46 ± 0.37	9.94 ± 0.21	83.60 ± 0.28
	24	ATO	3.67 ± 0.69	93.54 ± 2.30	2.79 ± 1.83
		HSA-ATO	8.41 ± 0.70	11.21 ± 1.12	80.39 ± 1.17
		FA-HSA-ATO	19.62 ± 1.27	10.81 ± 2.45	67.74 ± 2.48
U937	6	ATO	1.49 ± 0.25	95.25 ± 1.03	3.26 ± 1.24
		HSA-ATO	2.66 ± 0.60	10.65 ± 0.59	86.69 ± 0.32
		FA-HSA-ATO	6.17 ± 0.39	9.89 ± 0.99	83.95 ± 1.38
	24	ATO	3.49 ± 0.41	93.67 ± 0.77	2.84 ± 0.37
		HSA-ATO	8.12 ± 0.74	10.99 ± 0.91	80.89 ± 1.23
		FA-HSA-ATO	21.46 ± 2.21	10.86 ± 2.60	69.52 ± 1.43
A549	6	ATO	1.06 ± 0.06	96.44 ± 0.61	2.50 ± 0.66
		HSA-ATO	4.19 ± 0.56	10.19 ± 0.97	85.62 ± 0.80
		FA-HSA-ATO	8.84 ± 0.69	9.32 ± 0.95	81.84 ± 0.28
	24	ATO	2.85 ± 0.62	94.04 ± 1.02	3.11 ± 1.61
		HSA-ATO	10.00 ± 0.38	12.12 ± 1.00	77.88 ± 0.75
		FA-HSA-ATO	20.63 ± 1.36	12.15 ± 1.51	67.23 ± 2.55
H1299	6	ATO	1.06 ± 0.11	96.54 ± 1.18	2.40 ± 1.25
		HSA-ATO	4.36 ± 0.55	9.69 ± 1.08	85.95 ± 0.76
		FA-HSA-ATO	10.00 ± 0.86	9.24 ± 0.96	11.81 ± 1.62
	24	ATO	2.81 ± 0.44	94.49 ± 0.53	2.70 ± 0.72
		HSA-ATO	10.44 ± 0.83	11.22 ± 0.76	78.34 ± 0.14
		FA-HSA-ATO	24.53 ± 0.69	11.81 ± 1.62	63.67 ± 1.71
HeLa	6	ATO	1.01 ± 0.25	95.65 ± 1.48	3.34 ± 1.24
		HSA-ATO	4.78 ± 0.41	9.69 ± 0.80	85.53 ± 1.07
		FA-HSA-ATO	12.52 ± 1.49	9.57 ± 0.70	77.91 ± 1.00
	24	ATO	2.99 ± 0.93	93.93 ± 2.17	3.18 ± 1.36
		HSA-ATO	10.55 ± 0.66	10.88 ± 1.90	78.57 ± 1.85
		FA-HSA-ATO	30.86 ± 1.38	11.47 ± 0.78	57.67 ± 2.16
CCRF-CEM	6	ATO	1.14 ± 0.23	96.22 ± 0.52	2.65 ± 0.66
		HSA-ATO	2.50 ± 0.30	11.59 ± 1.99	85.90 ± 2.23
		FA-HSA-ATO	2.74 ± 0.62	11.79 ± 1.59	85.47 ± 2.20
	24	ATO	2.65 ± 0.61	94.97 ± 0.51	2.38 ± 0.69
		HSA-ATO	6.78 ± 0.85	11.53 ± 1.48	81.69 ± 1.25
		FA-HSA-ATO	7.41 ± 0.67	11.54 ± 0.95	81.05 ± 1.36
Ramos	6	ATO	1.23 ± 0.34	96.49 ± 0.37	2.28 ± 0.35
		HSA-ATO	2.55 ± 0.42	10.06 ± 0.95	87.39 ± 1.26
		FA-HSA-ATO	2.60 ± 0.46	9.38 ± 0.89	88.01 ± 1.34
	24	ATO	2.73 ± 0.58	94.51 ± 0.90	2.76 ± 0.50
		HSA-ATO	7.15 ± 0.43	11.43 ± 1.13	81.42 ± 0.81
		FA-HSA-ATO	7.65 ± 0.19	10.96 ± 1.20	81.39 ± 1.38

Table S4. IC_{50} of ATO, HSA-ATO and FA-HSA-ATO on 7 FRβ+ cancer cell lines and 2 FRβ- cancer cells after 72-h incubation.

Folate receptor expression	Cell	Tissue	ATO	HSA-ATO	FA-HSA-ATO	1 mM FA combination
	K562	Human chronic myeloid leukemia	10.97 ± 0.90	4.91 ± 0.98	2.32 ± 0.40	18.63 ± 4.21
	K562/ADR*	Human chronic myeloid leukemia	15.62 ± 1.07	5.36 ± 0.56	2.53 ± 0.28	—
	HL-60	Human acute promyelocytic leukemia	9.94 ± 1.09	4.62 ± 0.60	2.41 ± 0.32	—
	U937	Human acute myeloid leukemia	12.61 ± 1.50	6.50 ± 0.69	3.56 ± 0.35	—
FRβ+	A549	Human non-small cell lung cancer	16.84 ± 1.46	8.67 ± 1.03	4.12 ± 0.50	—
	HeLa	Human cervical cancer	18.25 ± 1.67	8.16 ± 0.71	3.74 ± 0.43	—
	H1299	Human lung carcinoma	17.92 ± 1.84	8.96 ± 0.95	4.42 ± 0.52	—
	CCRF-CEM	Human precursor T cell acute lymphoblastic leukemia	9.72 ± 1.31	4.89 ± 0.70	4.64 ± 0.56	—
FRβ-	Ramos	Human B cell Burkitt's lymphoma	9.84 ± 1.66	5.01 ± 0.63	5.19 ± 0.97	—

Notes:

1. IC_{50} was the half maximal inhibitory concentration.
2. Calculation of IC_{50} values was based on the concentration of arsenic.
3. Data were mean ± SD of three independent experiments.

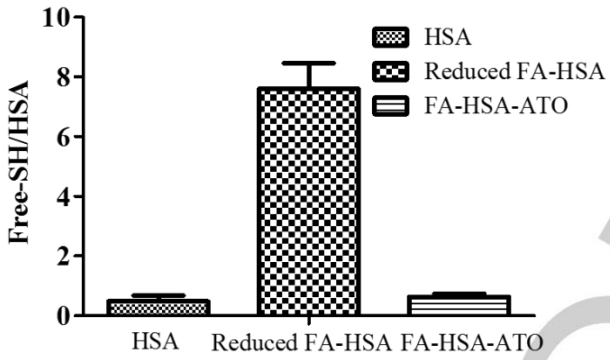

Figure S1. Analysis of free sulfhydryl ratio of the three HSA formulations.

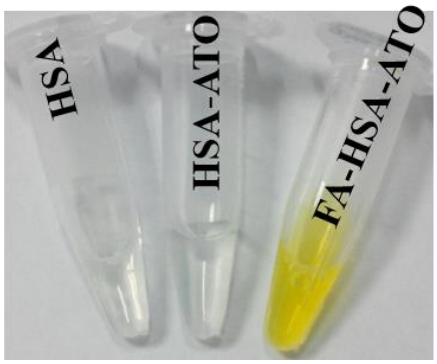

Figure S2. Optical image of HSA, HSA-ATO and FA-HSA-ATO in Dulbecco's phosphate buffered saline without Ca^{2+} and Mg^{2+}.

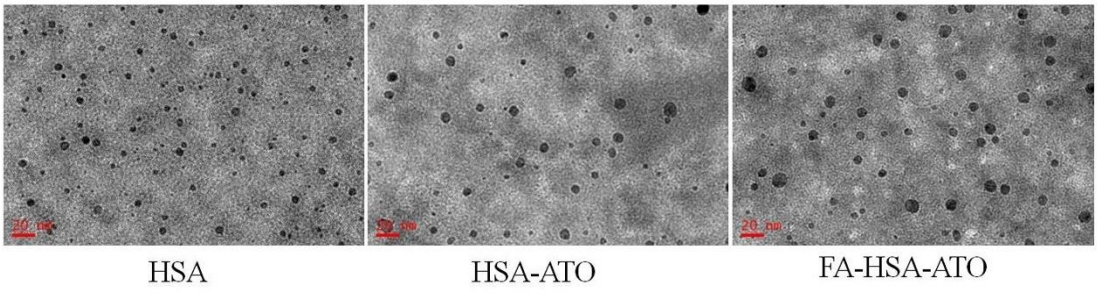

Figure S3. TEM images of HSA, HSA-ATO and FA-HSA-ATO. The samples were negatively stained with 2% phosphotungstic acid.

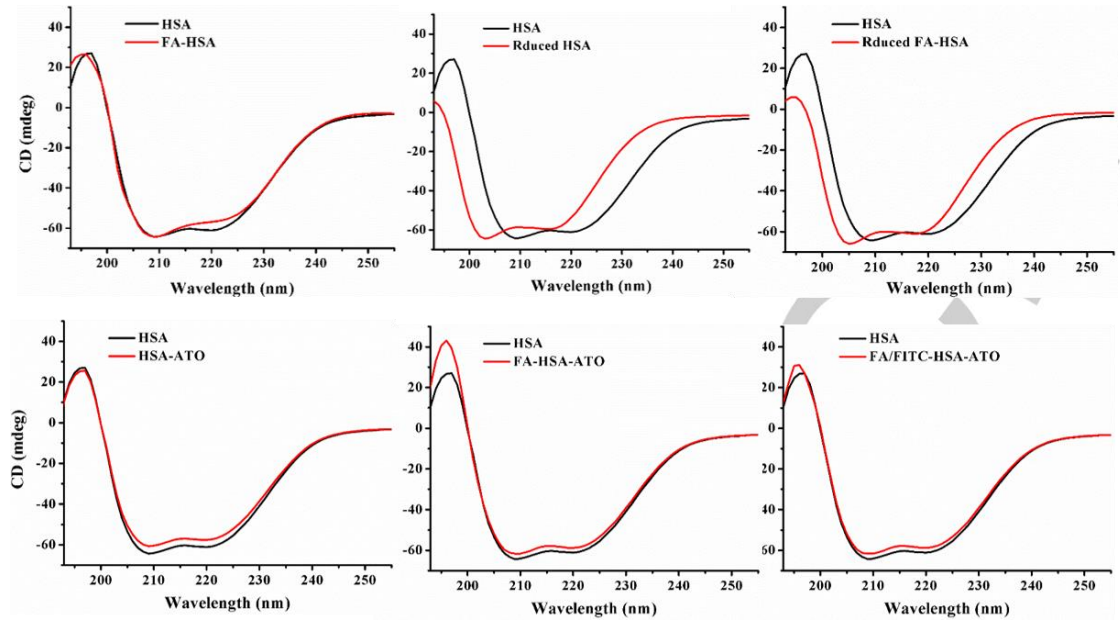

Figure S4. CD spectra of HSA, FA-HSA, reduced HSA, reduced FA-HSA, FA-HSA, HSA-ATO, FA-HSA-ATO and FA/FITC-HSA-ATO.

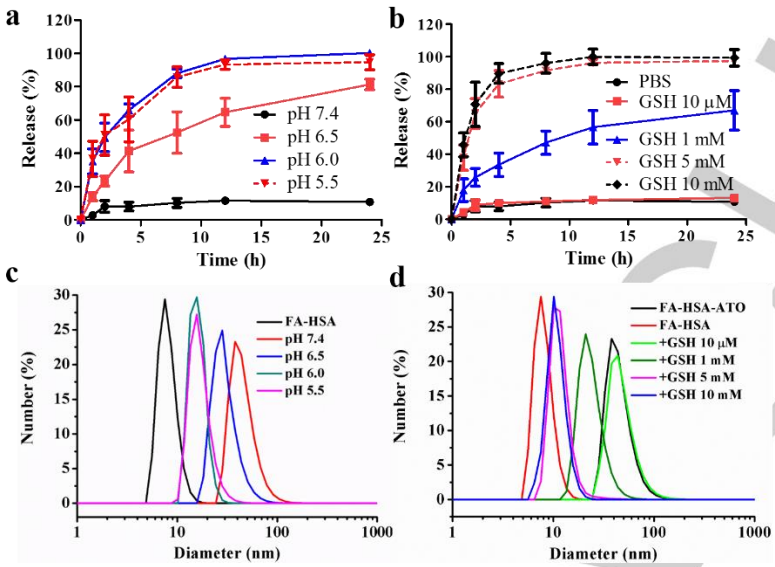

Figure S5. The kinetics of ATO release from FA-HSA-ATO in response to different pH (a) and GSH at different concentrations (b) at 37 ℃ (n = 3, bars represent means ± SD). The effect of pH (c) and GSH (d) on the hydrodynamic size of FA-HSA-ATO at 37 ℃.

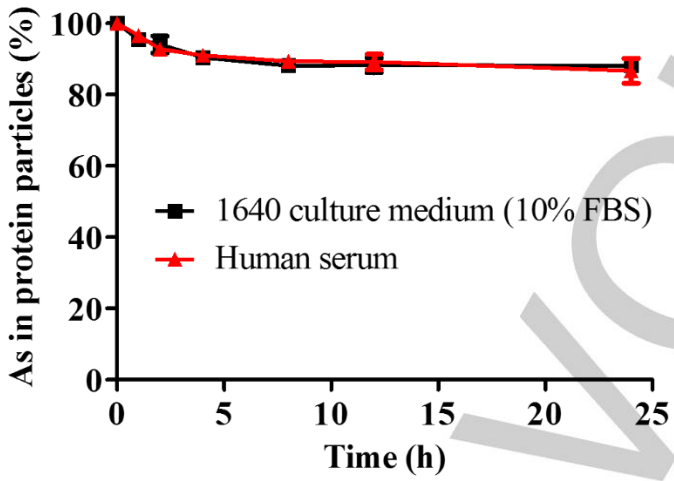

Figure S6. Stability of FA-HSA-ATO in 1640 culture medium, including 10% FBS and human serum, at 37 ℃ during a 24-h incubation (n = 3, bars represent means ± SD).

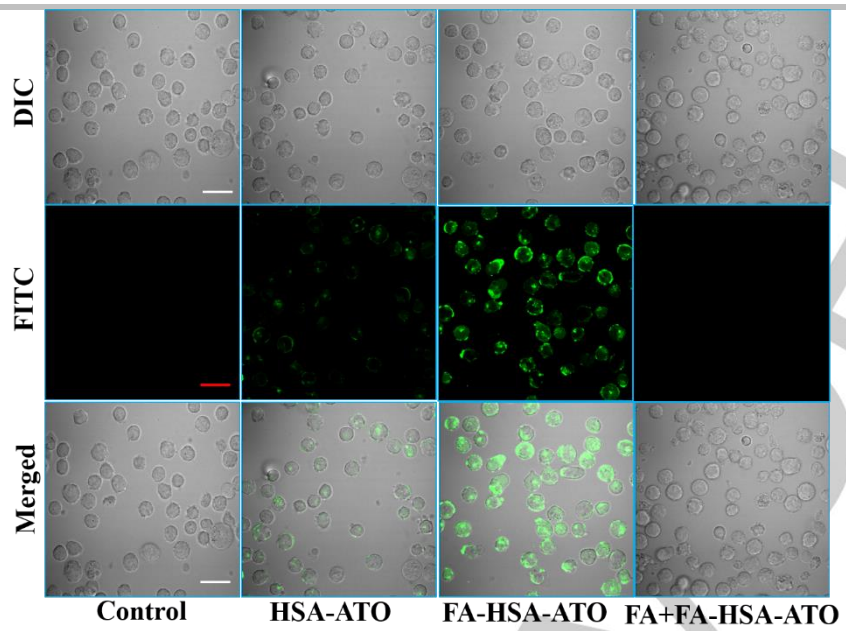

Figure S7. Confocal microscopy imaging of FR-β-targeting ability of FA-HSA-ATO (Scale bar = 30 μm).

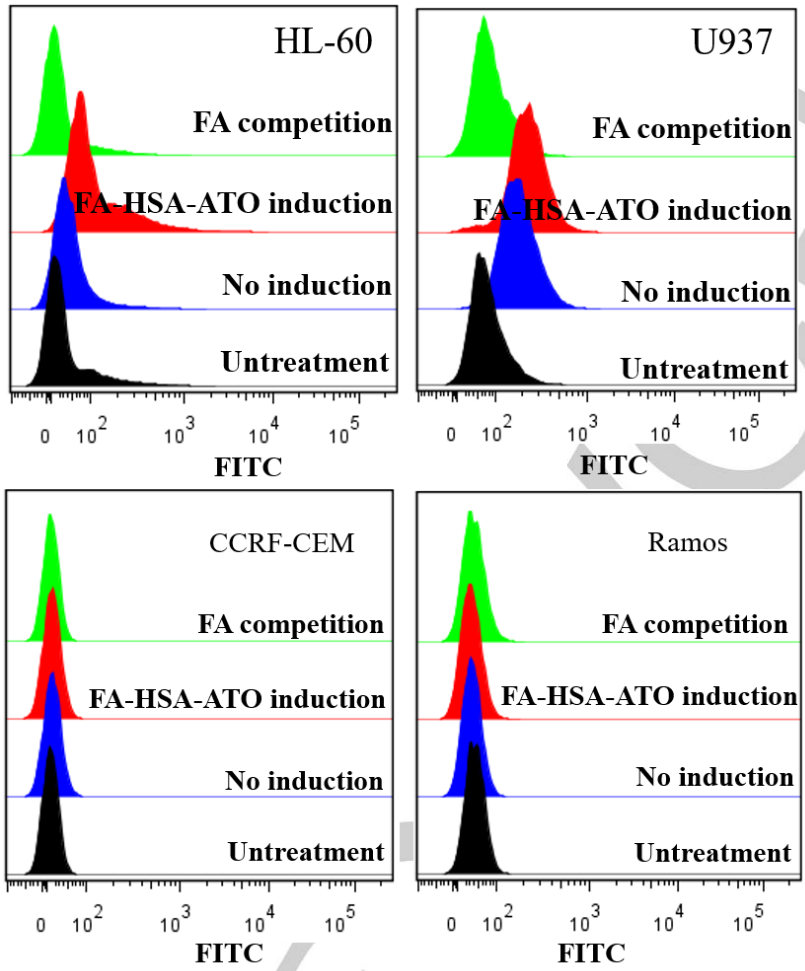

Figure S8. FA-HSA-ATO upregulated FR-β expression in a cell-dependent manner. FITC-PEG-FA, as the ligand of FR-β, was employed to detect the FR-β expression of cancer cells, and FA was used as competitive inhibitor of FITC-PEG-FA. HL-60, U937, CCRF-CEM and Ramos cells were treated with FA-HSA-ATO (1 μM As) for 72 hours, followed by the incubation of FITC-PEG-FA. The fluorescence values representing FR-β expression were detected by flow cytometry. For further validation, 1 μM FA was used to competitively bind FR-β before the addition of 10 nM FITC-PEG-FA.

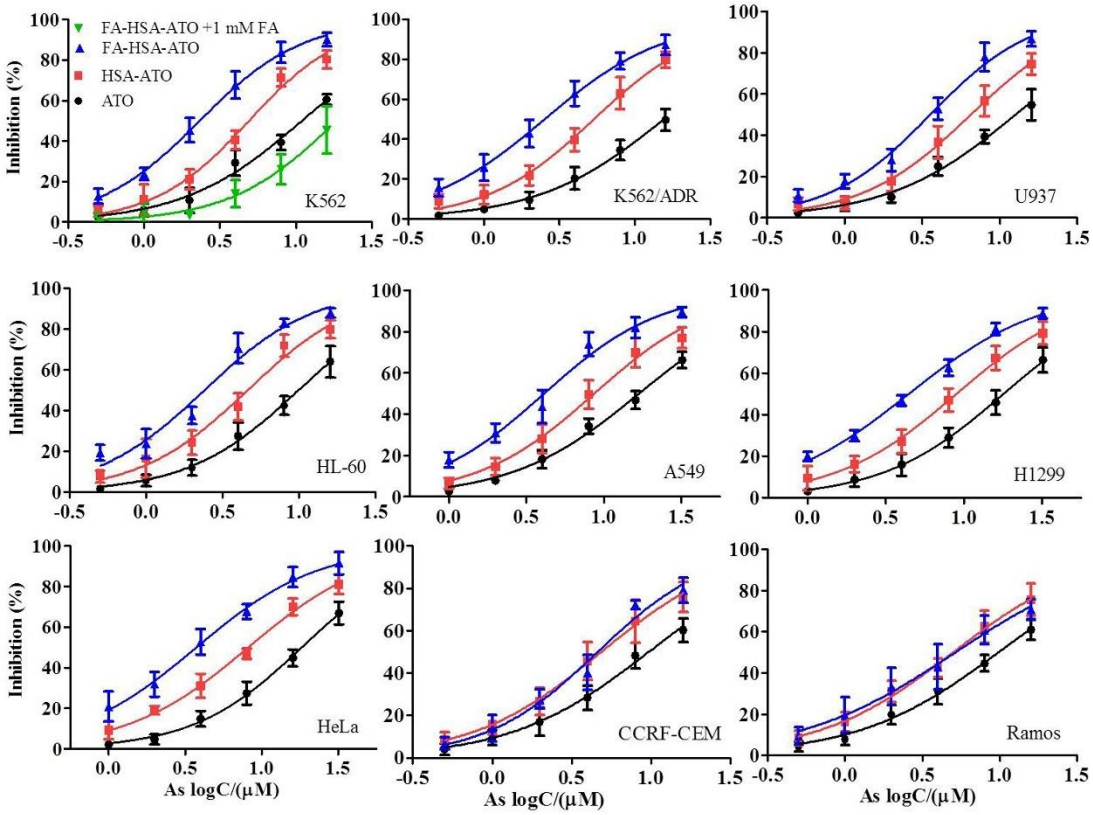

Figure S9. *In vitro* cytotoxicity of free ATO, HSA-ATO and FA-HSA-ATO against different cancer cells. Data are shown as mean ± SD (n = 5, bars represent means ± SD).

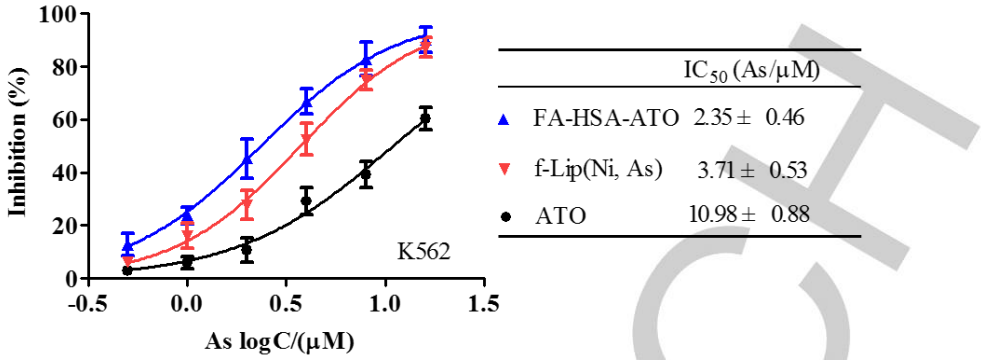

Figure 10. *In vitro* cytotoxicity of free ATO, f-Lip(Ni, As) and FA-HSA-ATO against K562 cells. Data are shown as mean ± SD (n = 5, bars represent means ± SD).

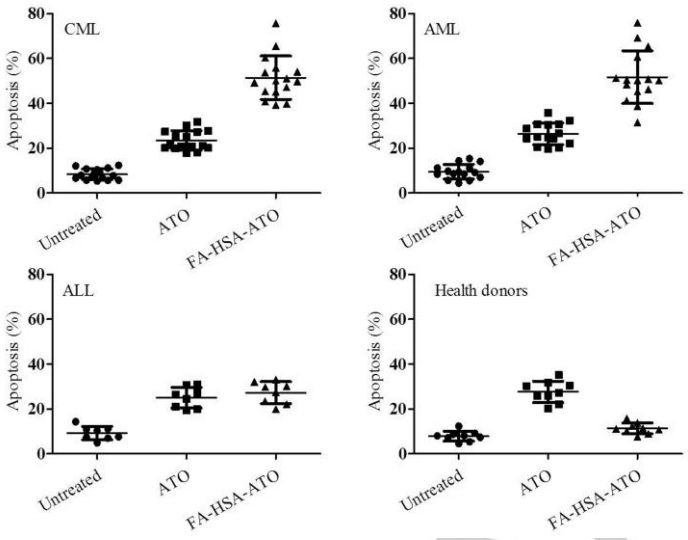

Figure S11. Cytotoxicity of FA-HSA-ATO against leukemia mononuclear cells from clinical patients and normal mononuclear cells from healthy donors.

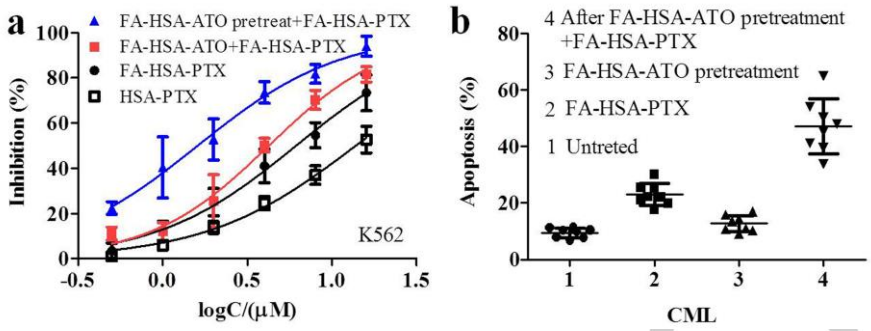

Figure S12. Cytotoxicity of FA-HSA-PTX against K562 cells and primary mononuclear cells from CML patients treated with or without FA-HSA-ATO.

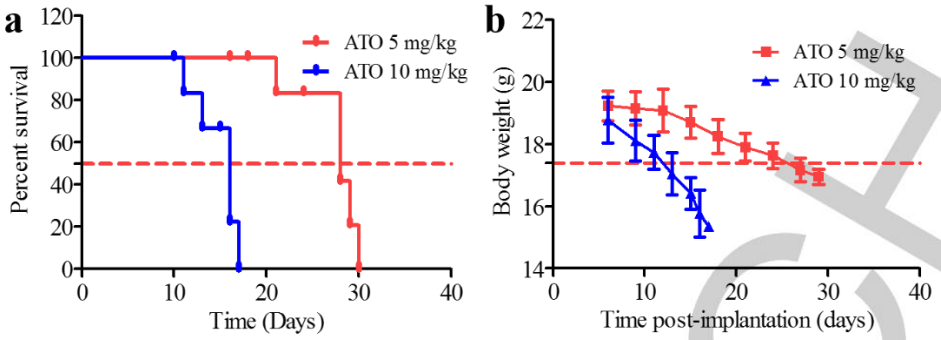

Figure S13. (a) Animal survival curves and (b) body weight changes in groups treated with ATO at 5 or 10 mg/kg/day (bars represent means ± SD, n = 5).

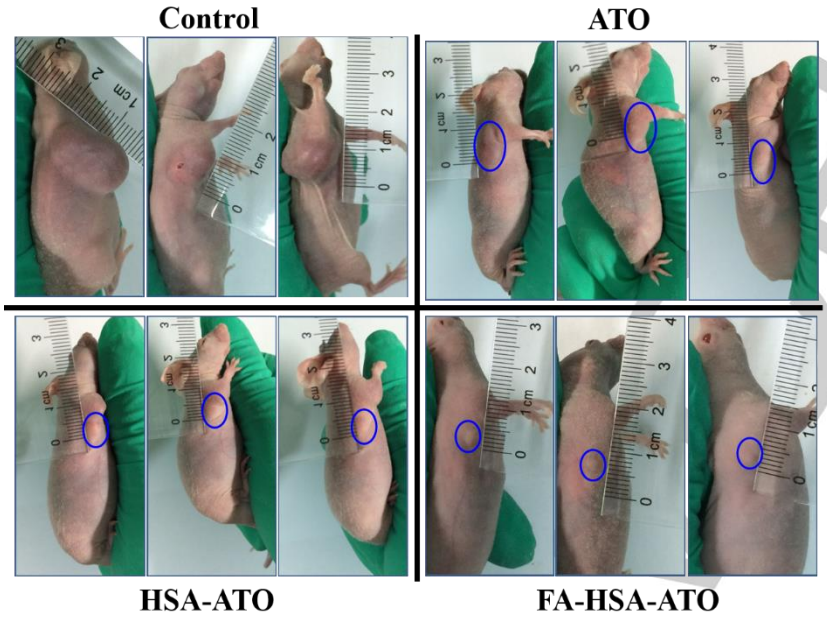

Figure S14. Photographs of mice on day 24 after treatments with HSA, free ATO, HSA-ATO and FA-HSA-ATO.

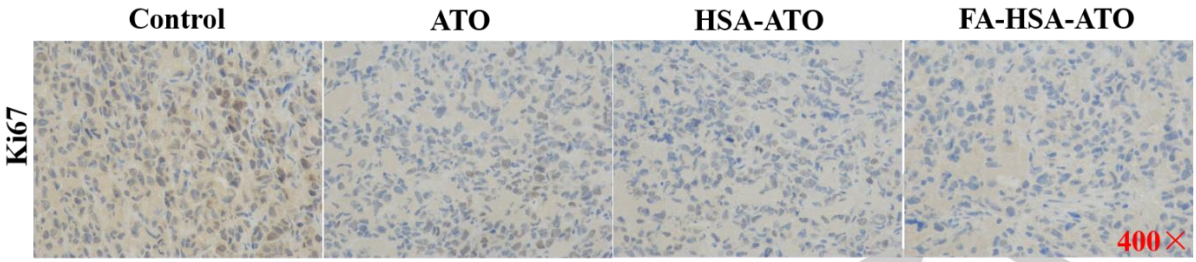

Figure S15. Representative immunohistochemistry staining of the proliferation marker Ki67 in tumor tissue sections, the results show that lower level expression of Ki67 in tumours after treatment with ATO, HSA-ATO or FA-HSA-ATO.

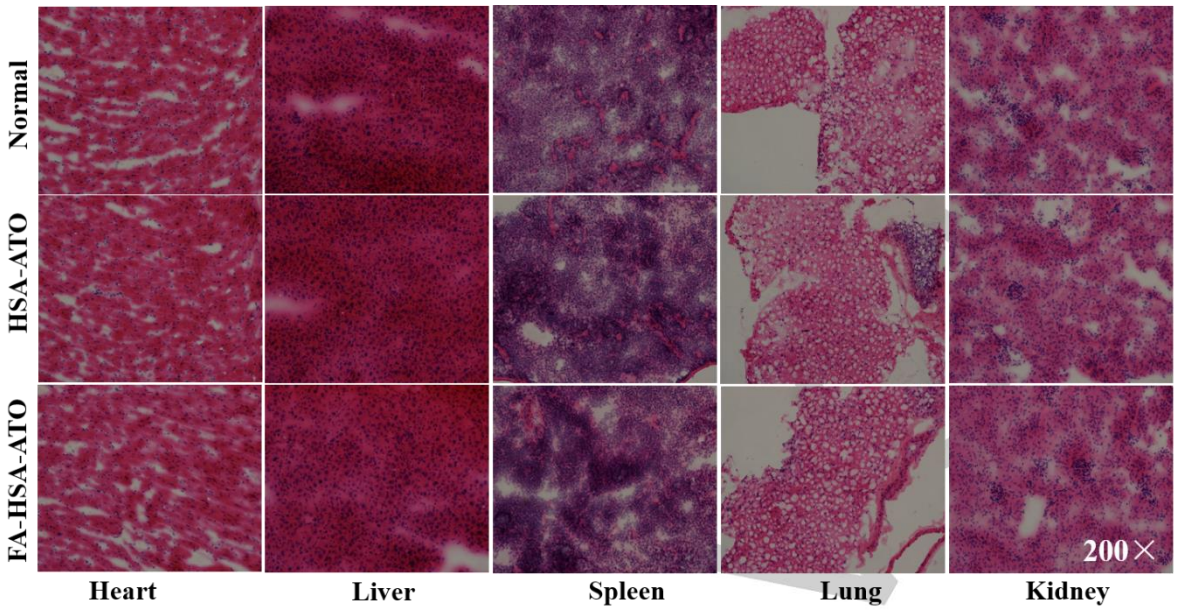

Figure S16. Representative H&E staining of major organ tissue sections with no evident systemic toxicity resulting from treatment with either HSA-ATO or FA-HSA-ATO.